

Investigation of wax and paper materials for the fabrication of paper-based microfluidic devices

Z. W. Zhong · Z. P. Wang · G. X. D. Huang

Received: 5 November 2011 / Accepted: 29 February 2012 / Published online: 13 March 2012
© Springer-Verlag 2012

Abstract Paper-based microfluidic devices hold great potential in today's microfluidic applications. They offer low costs, simple and quick fabrication processes, ease of uses, etc. In this work, several wax and paper materials are investigated for the fabrication of paper-based microfluidic devices. A novel method of using wax as a suitable backing to a paper-based analytical device has been demonstrated. Governing equations for the mechanics of the fluid flow in paper-based channels with constant widths have been experimentally validated. Experimental results showing deviations from the governing equations have been verified using fluidic channels with varying widths. There lies the possibility of manipulation of the fluid flow in paper-based microfluidic devices solely using geometric factors. This opens up many potential applications that may require sequential delivery of reagents or samples. Lastly, properties of paper such as the average pore diameter and permeability can be deduced from experimental results.

1 Introduction

Silicon and glass have been used as the substrate materials for microfluidic applications due to many of their good properties (Carlen et al. 2009; Coltro et al. 2007). Typical micromachining of silicon and glass involves dry and wet

etching, lithography and other techniques, all of which require clean room facilities and equipment (Fiorini and Chiu 2010).

Researchers have explored cheaper material alternatives such as polymeric devices (Ford et al. 2001; Zhong et al. 2011a), and novel fabrication techniques using polymers have been realised (Chartiera et al. 2003; Zhong et al. 2006). Polymeric microfluidic devices can be fabricated by a variety of techniques depending on the intended applications and the equipment available (Haiducu et al. 2008; Zhong et al. 2010). Polymeric materials of different grades and types are easily available, and the fabrication techniques have saved time and cost compared to glass and silicon-based devices (Song et al. 2004). For example, devices produced from poly methyl methacrylate (PMMA) have good properties and the production cost is low especially using commercial grade PMMA (Kaleibar et al. 2010). The cyclic olefin copolymer (Zhou and Papautsky 2007) is highly suitable for the fabrication of microfluidic devices using hot embossing (Yeo et al. 2010; Zhong et al. 2011b) techniques.

However, due to the emerging vast markets for analytical applications in the areas such as healthcare and food, researchers find even cheaper alternative materials for minimal costs, and the interests in paper-based microfluidic devices are increased in recent years (Martinez et al. 2007). Paper microfluidics was first achieved by patterning chromatography paper with polydimethylsiloxane (PDMS) or SU-8 (Lu et al. 2009). Recently, multi-level paper devices were developed, which opened up the possibility of running parallel tests on smaller devices (Lin and Lee 2010).

The main advantages of using paper materials are low cost, easy obtain-ability, high porosity, great biodegradability, and chemical compatibility with many applications (Martinez et al. 2008a). In addition, paper devices require minimal infrastructure, have simple and quick fabrication

Z. W. Zhong (✉) · G. X. D. Huang
School of Mechanical and Aerospace Engineering,
Nanyang Technological University, 50 Nanyang Avenue,
Singapore 639798, Republic of Singapore
e-mail: mzwzhong@ntu.edu.sg

Z. P. Wang
Singapore Institute of Manufacturing Technology,
Singapore, Republic of Singapore

processes, are easy to use, have the potential of remote usage and the ability to provide semi-quantitative test results in a point-of-care fashion (Martinez et al. 2008c). Moreover, paper can be easily patterned for high-volume fabrication of microfluidic paper-based analytical devices (mPADs), and the flow of samples in these devices can be achieved by the capillary action without using any external pumping systems (Coltro et al. 2010).

Using conventional photoresist materials to fabricate these devices has the drawback of having lower flexibility, and thus the devices can be easily damaged by bending and folding (Li et al. 2010). However, because of the lithographic process, the feature dimensions on SU-8 devices can be precisely controlled (Klasner et al. 2010). Hence, a photolithographic method called fast lithographic activation of sheets was introduced with a lower cost compared to the conventional lithography (Martinez et al. 2008b). A fabrication technique using a desktop plotter and a modified pen was also proposed without the need for a clean room (Coltro et al. 2010). The devices can also be fabricated by inkjet printing, and the detecting reagents can be applied to the test zones by printing (Klasner et al. 2010).

Fabrication with wax is to penetrate wax through the paper depth to define hydrophilic microchannels on the paper substrate. This technique gives a cheaper and more convenient alternative than traditional patterning of SU-8 or PDMS onto the paper substrate (Lu et al. 2009). The smallest hydrophobic barriers achieved are ~ 850 μm in width with an edge roughness of about 60 μm , and the smallest hydrophilic channels are ~ 560 μm in width (Carrilho et al. 2009). Solid wax printing has many advantages such as quick fabrication, no need for extra processing steps, and the ability to print barriers of various colours (Martinez et al. 2010).

This work was to investigate a microfluidic platform that is economical, provides ease of use, and has the prospect of mass production for potential “use and discard” applications. The focus was on the science of paper-based devices that offer very low cost and minimum energy consumption. Feasibility of using wax as a suitable substance for the formation of hydrophobic barriers was investigated. Paper properties such as permeability and the average pore diameter were determined through experimental techniques. Theoretical mechanics of the fluid flow in porous media was validated by experimental results of the fluid flow in paper devices.

2 Wax for paper-based devices

2.1 Paper substrates and wax

This experiment was to test the wicking capabilities of different types of paper substrates, and the compatibility of

different types of wax with the paper substrates. The paper substrates tested were A4-sized printing paper, kitchen towel, thin paper napkins, and laboratory paper (paper towel used in laboratories). The wax types tested were wax/grease pencils, wax crayons, candle wax, and lipsticks.

Desired channel patterns were drawn on both single and double sides of the paper substrates using a wax pencil, wax crayon or lipstick. The channel widths before wax diffusion were 5 and 10 mm, and the channel length was 4 cm. The patterned paper was heated at 150 °C on a hot plate for 2 min. Then sufficient coloured water was pipetted to completely fill up one “reservoir” of the pattern to allow sufficient pressure for capillary action along the channel. Subsequently, the device was left on a horizontal platform for observation. When candle wax was tested, the steps were similar except that there was an additional wax melting step before patterning of the paper substrates. This was achieved by breaking candles into smaller bits, followed by heating the candle bits to the liquid form. The patterning was then achieved using a paintbrush.

Experiment results show that the laboratory paper and paper napkin are able to transport the liquid from one “reservoir” to the other within 30 s. The printing paper has low “wicking” capabilities, due to the low porosity level and surface tension effects of the paper, making it unsuitable for liquid transport. Having high porosity may not be ideal for liquid transport as the diffusion of wax barriers through the paper may be adversely affected, as was demonstrated by the kitchen towel where due to uneven and incomplete diffusion of wax barriers, the liquid cannot be fully constricted within the boundaries of the channels and “reservoirs”.

Both the laboratory paper and paper napkin have good “wicking” capabilities with the most rapid and reliable being the laboratory paper. Liquid transport from one “reservoir” to the other requires 10 s or less. Although the paper napkin has good liquid transport, there was considerable leakage along the channel length due to the thinness of the paper napkin. This may cause problems of contamination or lost samples in actual applications. Further tests to examine the anisotropic nature of the alignment of the fibres revealed that the liquid could still be transported if the channels were drawn in different directions from the layout of the fibre on the paper substrates.

Wax crayons can diffuse through the laboratory paper forming wax barriers. However, the effectiveness of the wax diffusion is limited as the tip of the wax crayon may be too brittle, thus impeding well-defined patterning on the substrate. The brittleness of the wax crayon tip together with the highly porous structure of the kitchen towel makes the diffusion of wax barriers ineffective. However, the ingredients used in wax crayons can form suitable hydrophobic barriers on paper substrates.

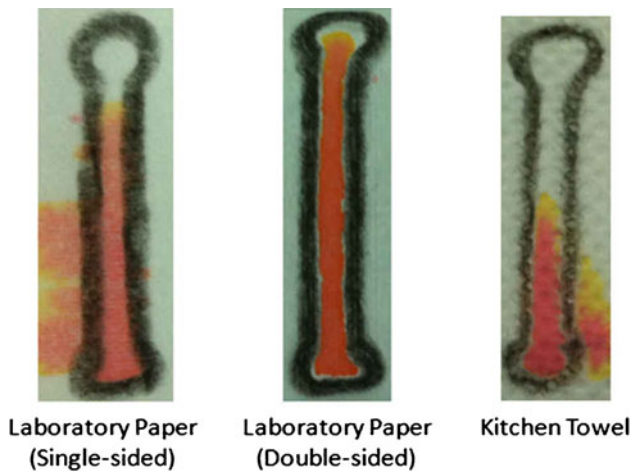
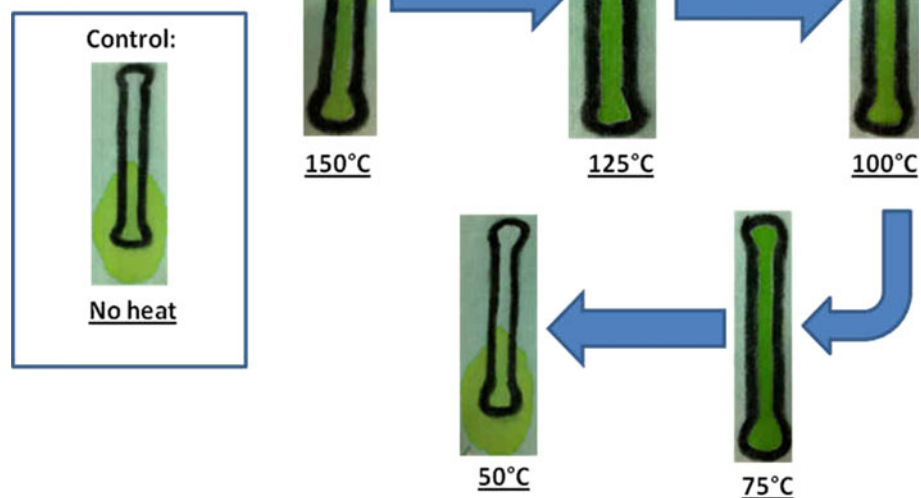


Fig. 1 Wax channels patterned on paper substrates using a wax pencil

A wax pencil was used to pattern channels on paper substrates with three setups: draw on a single side of the laboratory paper, draw on both sides of the laboratory paper, and draw on both sides of the kitchen towel. Figure 1 shows that the wax pencil is suitable for wax diffusion to form hydrophobic barriers on paper substrates. This can be seen from the double-sided setup whereby the liquid flows smoothly from one “reservoir” to the other without any leakage. If only one side of the paper is patterned with wax, wax diffusion may not be complete throughout the pattern, thus causing leakage at certain portions of the channel. Incomplete wax diffusion is observed on the porous kitchen towel.

Fig. 2 Wax barriers for containing *green-coloured* water at various temperatures



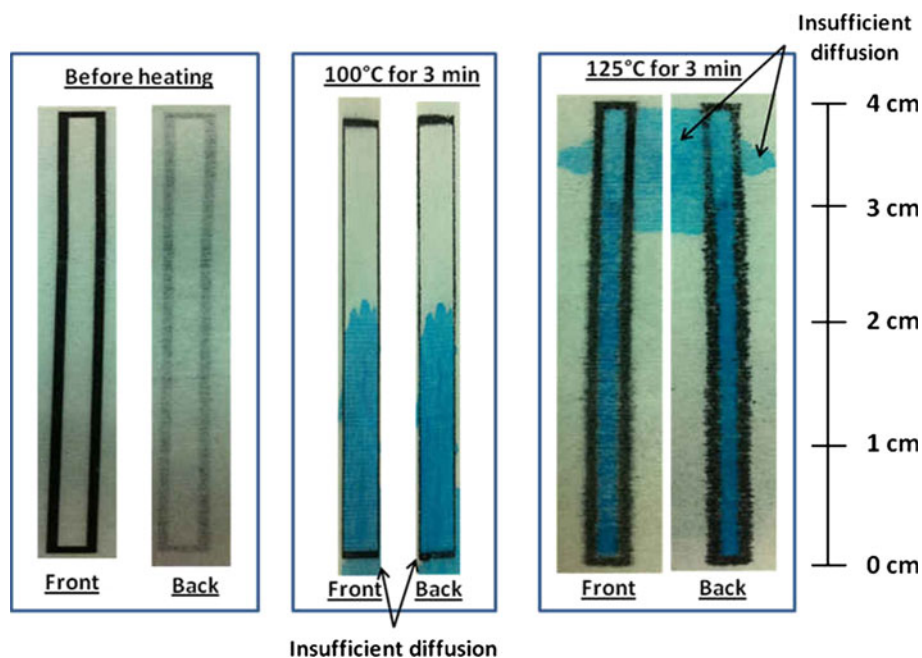
The effectiveness of the candle wax on the laboratory paper was also investigated. The heat treatment caused the candle wax to diffuse rapidly in all directions throughout the paper. This caused the defined channel to be totally covered by transparent wax, hence restricting any kind of liquid transport. The entire area surrounding the candle wax was considered hydrophobic after heat treatment. Further experiments were carried out by enlarging the channel width but wax diffusion of the candle wax was simply too rapid, making it impossible to achieve proper definitions of the channels. Similar tests were also performed using a lipstick and the same results were obtained.

2.2 Effective temperature for wax diffusion

This experiment was to identify the minimum temperature required for wax diffusion throughout the depth of the paper substrate. Channels were drawn on both sides of the laboratory paper substrate using a wax pencil. The substrate was then heated at a temperature on a flat plate for 2 min.

As shown in Fig. 2, the wax barriers can sufficiently contain the green-coloured water within the channel if the paper substrate is heated at 75 °C and above. At 50 °C, the wax fails to completely diffuse throughout the depth of the paper, hence rendering the hydrophobic barriers ineffective. The coloured water does not wick within the channel. The melting point of the wax used in the wax pencils is between 50 and 75 °C. 75 °C is a suitable temperature for wax diffusion to suffice for the creation of hydrophobic barriers on paper substrates. Another observation is the “curling” up of the paper upon heat exposure

Fig. 3 Printed wax channels before diffusion and the results of fluid flow tests performed using the channels



of 150 °C and above. Thus, the range for heat exposure should be kept between 75 and 125 °C.

2.3 Solid ink printing

A solid ink printer was used to print wax on the laboratory paper, followed by heat treatment of the paper substrate on a hotplate to allow wax diffusion throughout the depth of the paper. Figure 3 shows the printed wax channels before diffusion and the results of the fluid flow tests performed on the channels that were exposed to a hotplate temperature of 100 or 125 °C for 3 min. Before heat treatment, the wax only adhered to one side of the paper. The heat treatment allowed wax diffusion to penetrate throughout the paper depth. The channel width was 1 mm. Blue-coloured water was introduced to the channels at the 0-cm mark and flowed towards the other channel ends, i.e., the 4-cm mark. At 100 and 125 °C, the fluid was transported within the boundaries of the barriers for most parts of the channels. At 125 °C, leakages out of the channel boundary only occurred between the 3 and 4 cm marks, as wax diffusion was incomplete at certain portions of the channels. A longer heat exposure time may solve the problem of incomplete diffusion. Another possible reason may be the uneven surface on the hotplate or the “curl-up” of paper during heating. Using suitable paper weights to apply pressure during heating may help to ensure even meshing between the surfaces of the paper and the hotplate.

Solid ink printing is suitable for the fabrication of wax-based mPADs. This offers higher consistency, accuracy and resolution, compared to hand-drawing using a wax pencil. However, the wax used in solid ink printing has a

higher melting temperature and requires a longer heat exposure time compared to the wax in a wax pencil. This implies that the time duration allocated for heating of the paper substrate must be increased when fabricating the mPAD using a solid ink printer.

2.4 A switch

One of the requirements for fluid manipulation is to incorporate a switch or valve into the fluidic device. The ability to control the fluid flow helps to materialise many microfluidic applications. The work reported in this section explores a possible prototype of a switch that may be a stepping stone to the future development of more complex and efficient paper-based microfluidic switches.

Channels having a length of 3 cm were drawn on both sides of the paper substrate using a wax pencil. Rectangular holes with widths of 5 mm were cut out somewhere midway of the channels. A paper strip with a width of 5 mm was then patterned using a wax pencil in such a way that the undrawn area had the same width as the fabricated channels. Both the channel and paper strip were heated on a flat plate to allow wax diffusion. After heating, the paper strip was inserted into the cut-out areas of the paper device. The fluid flow test was conducted in a set-up whereby the hydrophobic channel was activated, i.e., an open switch. As soon as the fluid flow was successfully constricted within the first half of the channel, the hydrophobic barrier was deactivated to allow fluid flow in the channel, i.e., a closed switch.

A simple “pull” on the paper strip can act as a switch that restricts or allows the fluid flow through the fluid

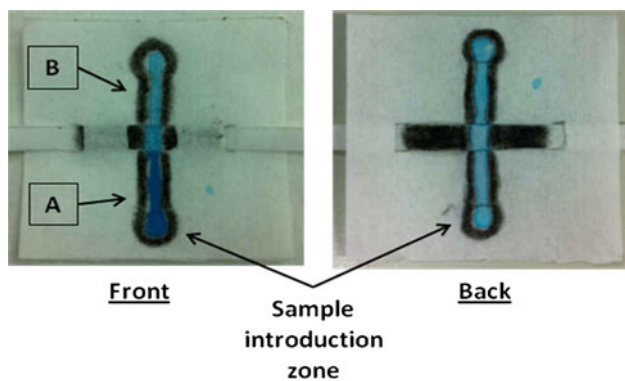


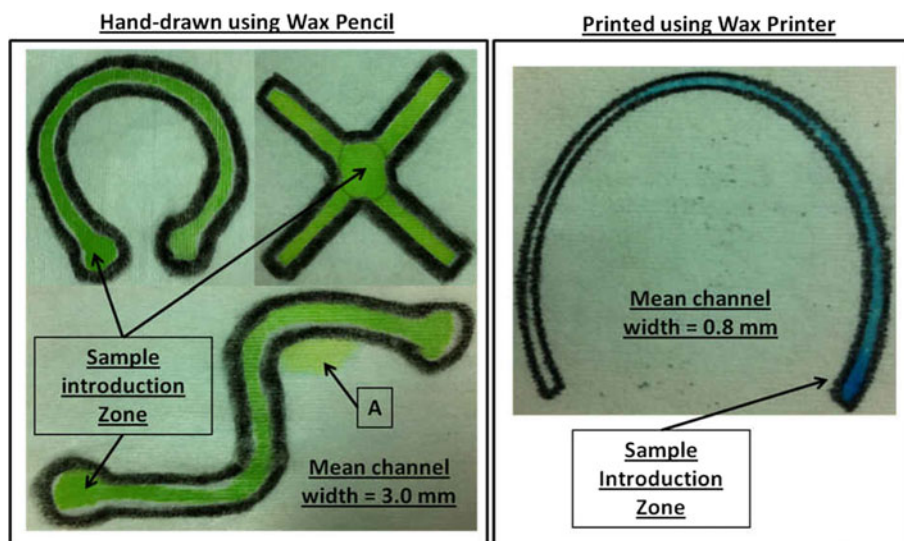
Fig. 4 A fluid test using the switch

channel. Figure 4 compares the colour intensity of sections A and B, which are the channels before and after the switch respectively. The fluid colour in section A is more intense, meaning that there is more fluid present in the region before the switch. The fluid was restrained within the first part of the channel when the hydrophobic barriers were activated. Logically, section A would then hold more fluid than section B. This experiment proves that the idea of a switch in a paper-based device is feasible. Further modifications to the design can be explored for various applications.

2.5 Designs of varying geometry

There is a need to test the feasibility of paper-based devices consisting of more complex geometry, i.e., curved, multiple channels. Figure 5 shows such channels fabricated using a wax pencil and the wax printer, which could contain the fluid flow within the wax boundaries. The fluid flow is indeed possible in curved and linear channels, and single or multiple channels, showing the possibility of

Fig. 5 Designs with varying geometry and shapes



fabricating more complex paper devices for various applications.

However, in the section labelled A, there was a fluid leakage out of the channel boundary, because the device was placed on a hydrophilic material (paper) during the experiment. This caused some of the fluid to flow onto the hydrophilic backing, subsequently spreading out in the lateral direction, and in turn to flow back onto the device.

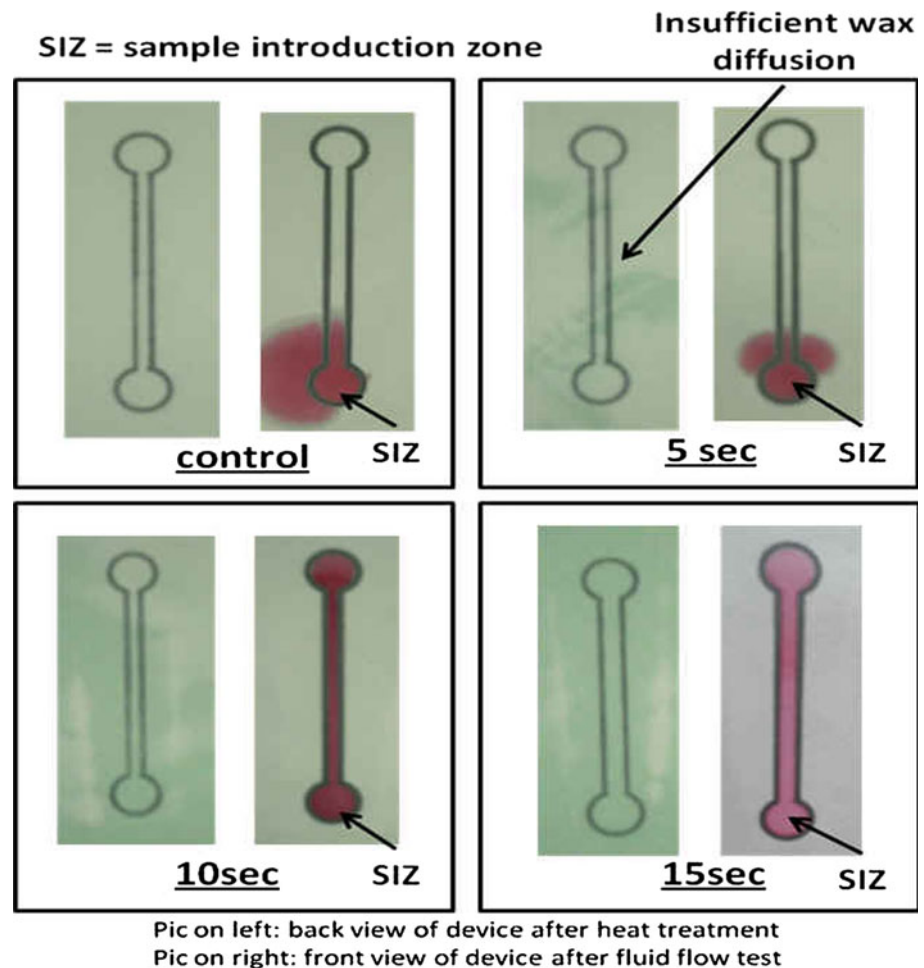
This suggests that there is a need to explore ways to provide a backing that is of hydrophobic nature. Devices can be designed in a way that they can be mounted onto thin acrylic plates that provide suitable backing to the paper devices. An alternative is to laminate the back of the paper device with a thin layer of polymer sheet. However, all these methods will increase the cost of production. Hence, a novel idea of using wax as a suitable backing was explored, and this is presented in the next section.

2.6 Wax as a backing

The feasibility of using wax as a hydrophobic backing was investigated for paper-based devices. Experiments were conducted to find the optimum heat exposure time required for wax to be precisely diffused laterally without diffusion through the paper depth. This investigation is crucial as under-exposure will cause the wax backing to be ineffective and an over-exposure will render the channel hydrophobic.

The wax printer was used to pattern the channels on the paper substrate followed by a 5 min heat treatment at 125 °C. Chromatography paper was chosen, as its fibre arrangement was more consistent compared to the previously used paper towels. After the fabrication of the channels, the paper substrates were left at room temperature for at least 10 min before applying a layer of wax on the back-side of the paper device using the wax printer. For

Fig. 6 Tests of the heat exposure time for wax to be a backing



the wax layer on the back of the device, a shade of grey colour (RGB model Red-202, Green-212, Blue-211) was chosen to clearly distinguish the wax between the channels (black) and the backing (grey). Subsequently, four different set-ups were carried out to find the optimum heat exposure time. The hot-plate temperature was 125 °C for all set-ups, and the heat exposure time was 0 (control set-up), 5, 10 and 15 s. These channels were then placed onto a piece of hydrophilic paper before the fluid flow test.

As shown in Fig. 6, both the control set-up (no heat exposure) and the set-up with a heat exposure of 5 s have insufficient wax diffusion, causing the wax layer at the back of the device to fail. This is depicted by the presence of fluid contamination between the paper device and the paper layer supporting the device. Some form of wax diffusion is evident in both set-ups for 10 and 15 s heat exposure times, as depicted in the left picture of both set-ups whereby the darker shade is evidence of wax diffusion of the grey wax on the back-side of the device. These set-ups could transport the fluid successfully without any contamination through the hydrophilic paper.

Other set-ups with heat exposure times of 20 s and above were also tested, and some portions of the fluid channels were rendered hydrophobic due to the rapid diffusion of the “wax backing” through the depth of the paper. At a heat exposure of 125 °C on a hotplate, the optimum exposure time for a paper device with a wax-based backing fabricated through the wax printer lies between 10 and 15 s.

3 Mechanics of fluid flow

3.1 Paper wet-out

The wet-out process describes the period when the porous matrix is originally clear of liquid. For the one-dimensional flow in a porous matrix like a paper strip, the fluid flow follows the Washburn equation (Fu et al. 2011),

$$L = \sqrt{\frac{\gamma Dt}{4\mu}} \quad (1)$$

where L = the distance moved by the fluid front, γ = the effective surface tension of the liquid, D = the average pore diameter, t = time, and μ = the viscosity of the liquid. The application of the Washburn equation for the flow in a porous media is based on the assumption that there is a non-limiting source and a constant cross-sectional area is maintained throughout.

3.1.1 Flow in constant-width channels

Experiments were conducted using paper-based fluidic channels with a constant width of 1.2, 1.6 or 2 mm, fabricated by wax printing. Grade 1 chromatography paper was used as it had the highest consistency in terms of fibre alignment and the flow rate. A video camera was used to record the entire flow processes. The video files were then converted into pictures at different time points, for measuring of the distances travelled by the fluid fronts. The results of the test are presented in Fig. 7, which clearly show that the flow characteristics are similar regardless of the width of the fluidic channels. In addition, the structures of the three curves suggest that the flow rates of the fluid fronts indeed follow the Washburn equation in the sense that the distance travelled by the fluid front is proportional to the square-root of time, i.e., $L \sim t^{0.5}$.

Slight variations in the different curves can be due to the following reasons: (1) small differences in the pore sizes of different paper samples, (2) the presence of small impurities in the paper matrix, and (3) the inconsistency in the diffusion of wax during the channel fabrication process that creates small differences in the driving force of the fluid.

Also, from the results gathered, we can deduce the average pore diameter (D) of the chromatography paper using the rearrangement of Eq. (1):

$$D = \frac{(4L^2\mu)}{\gamma t} \tag{2}$$

The surface tension and viscosity of water at the room temperature are 0.0728 N/m and 1.002×10^{-3} Ns/m²,

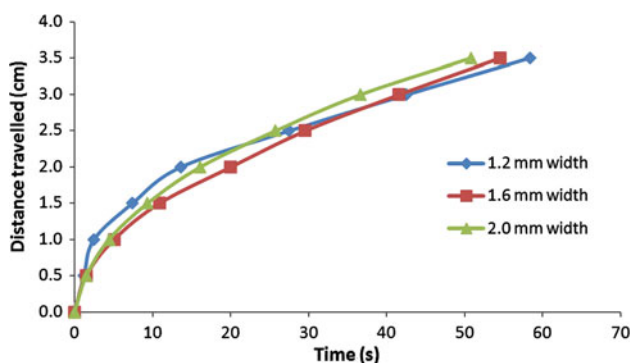


Fig. 7 Flow characteristics for the fluid flow in the channels of constant widths

respectively. Using these values and the results from the experiments, a deduced value of the average pore diameter can be obtained for each measurement taken. With the removal of the outliers below the lower control limit (LCL, the value 1 σ below the mean value) and above upper control limit (UCL, the value 1 σ above the mean value), the average pore diameter of the paper can be deduced by taking the mean of the remaining values. From this test, the average pore diameter of the paper is deduced to be 1.2 μm .

3.1.2 Constricted flow

A constricted fluid flow refers to a flow from a channel with a smaller width to another channel with a larger width. The word “constricted” is used because a flow from a channel with a smaller width to another one with a larger width violates the assumption of a non-limiting source. The fabricated channel with a fluid front at the 2.4 cm mark is shown in Fig. 8. Two designs of varying channel widths shown in Table 1 were tested, and both had a small-to-big transition at the 2 cm mark.

As shown in Fig. 9, the flow characteristics for both designs are very similar for the first half of the channels, i.e., before the transition point. This again shows that the liquid flow in a channel is independent of the channel width. However, after the transition point, both the flow rates depicted by the gradients of the curves are greatly decreased, because there is a constriction of the flow at the transition from a smaller-to-larger channel width. This

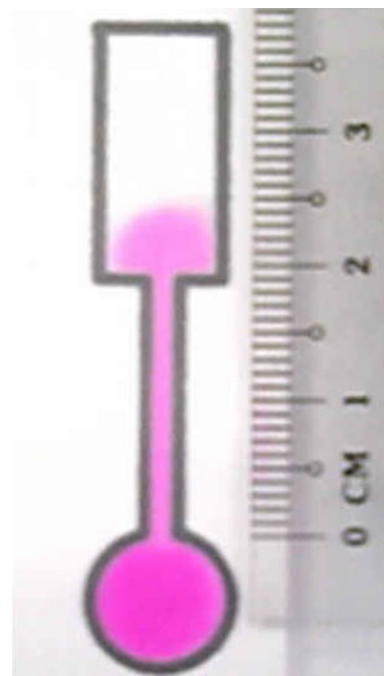
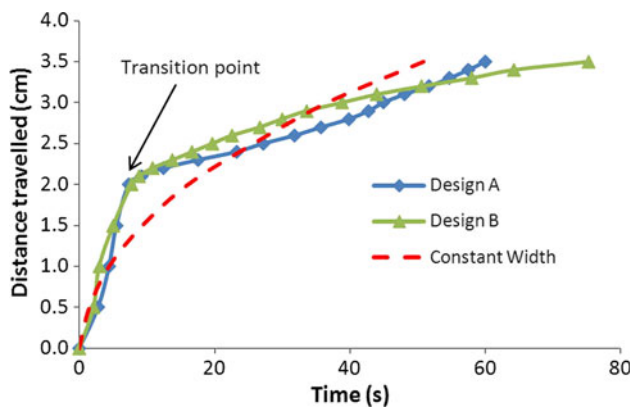


Fig. 8 The constricted fluid flow in a varying-width channel with a fluid front at the 2.4 cm mark

Table 1 Design specifications of the channels for constricted flow tests

Design	Smaller width (mm)	Larger width (mm)
A	1	8
B	2	8

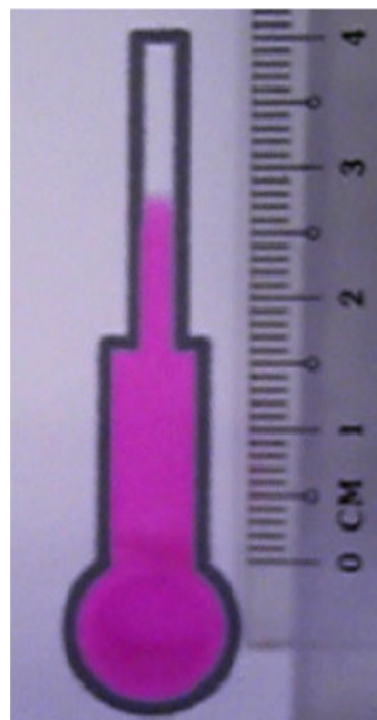
**Fig. 9** Flow characteristics of the constricted flow

observation is analogous to the principle of conservation of mass flowing along a channel. If a volumetric flow rate is conserved and the flow cross-sectional area increases due to an increase in the channel width, the flow rate of the fluid front must be decreased. In addition, by comparing the gradients of the curves in Fig. 9 for designs A and B just after the transition point, it is clear that design B results in a higher flow rate compared to design A. This observation again substantiates the principle of conservation of mass, as the first half of the channel in design B has a larger width than that in design A.

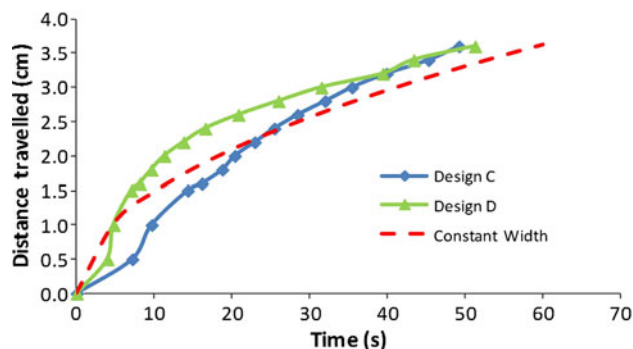
3.1.3 Abundant flow

An abundant flow refers to a flow from a channel with a larger width to another channel with a smaller width. The word abundant is used because a flow from a channel with a larger width may be considered a non-limiting source to the flow in a channel with a smaller width. A fabricated channel with a fluid front at the 2.8 cm mark is shown in Fig. 10. Two designs of varying channel widths shown in Table 2 were tested, and both had a big-to-small transition at the 1.6 cm mark.

As shown in Fig. 11, the trends of the curves for designs C and D are similar to that of the curve for a constant width design, i.e., $L \sim t^{0.5}$. It takes about the same time for the fluid fronts to travel a distance of 3.5 cm. This shows that the change in the channel width at the 1.6 cm mark does not affect the fluid flow rate, as there is sufficient liquid for

**Fig. 10** The abundant fluid flow in a varying-width channel with a fluid front at the 2.8 cm mark**Table 2** Design specifications of the channels for abundant flow tests

Design	Smaller width (mm)	Larger width (mm)
C	1	5.8
D	2	5.8

**Fig. 11** Flow characteristics for the abundant flow in varying-width channels

the flow to be sustained after the transition point. This observation validates the fact that a flow from a larger width channel can in fact act as a non-limiting source for the flow entering into a smaller width channel.

3.2 Fully wetted flow

A fully wetted flow refers to the flow characteristics of a fluid introduced into a pre-wetted channel, i.e., there exists the presence of fluid particles within the pores of the porous matrix. The flow characteristics for such flows can be described by Darcy’s Law given by (Fu et al. 2011),

$$Q = -\frac{\kappa WH}{\mu L} \Delta P \tag{3}$$

where, Q = the volumetric flow rate, κ = the permeability of the paper to the fluid, μ = the viscosity of the fluid, WH = the area of the channel perpendicular to the flow, and ΔP = the pressure difference along the flow direction over the length L . Assuming a constant cross-sectional area throughout and by division of WH on both sides of the equation, the flow rate of the fluid, q can be derived from Eq. (3) as,

$$q = -\frac{\kappa}{\mu L} \Delta P \tag{4}$$

3.2.1 Constant-width channels

Constant-width channels were fabricated by wax printing on chromatography paper. The fluidic channels were first pre-wetted with clear water before the test with coloured water. The entire process of the fluid flow was captured using a video camera. Three channels of different widths were tested, and the results are presented in Fig. 12.

As depicted in Fig. 12, the fluid flow curves for all three channels are very similar and the characteristic of the fully-wetted flow is independent of the channel width. This result is in fact consistent with the theory for the flow rate in a channel with a constant width.

According to the principle of conservation of mass, it is clear that the volumetric flow rate, Q , is constant along a channel. Thus, if the channel width is kept constant, the time taken for the fluid front to travel a certain distance can be calculated as (Fu et al. 2011),

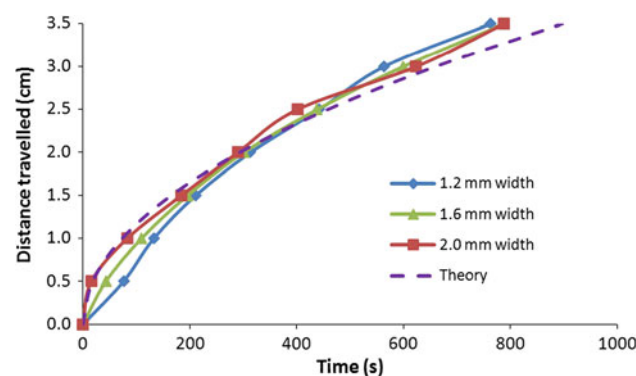


Fig. 12 Flow characteristics for the flow in constant-width channels

$$t = \frac{V}{Q} = \frac{V\mu L}{\kappa WH \Delta P} = \frac{\mu L^2}{\kappa \Delta P} \tag{5}$$

where V = the volume of the fluid at the time instant t .

The viscosity of water at the room temperature is assumed to be 1.002×10^{-3} Ns/m². As the pressure variation in a stand-alone paper-based device is driven solely by the capillary pressure within the pores, ΔP can be assumed to be a constant. For this test, ΔP is assumed to be 4,560 N/m² (Fu et al. 2011). Hence if the permeability of paper is assumed to be a constant, the only variable that affects the flow rate of the fluid is the geometric factor, i.e., if the thickness and width of the paper channels are kept constant, the time taken for the fluid flow is affected solely by the length L .

Under the above assumptions, the theoretical flow characteristic for a fluid flowing in a constant width paper channel, as presented in Fig. 12, can be developed through repetitive iterations of the constant κ . The deduced value for the permeability of a Grade-1 chromatography paper is 3×10^{-13} m². This deduced value is consistent with the range of experimentally deduced permeability for different grades of papers reported by Nilsson and Stenstrom (1996).

3.2.2 Varying-width channels

This experiment was conducted to understand the flow rates of the fluid in channels with varying cross-section dimensions and the same overall length (4 cm). Figure 13 shows two fluid channels with the flow fronts at the 1.5 cm mark. The smaller channel width is 1.2 mm and the larger width is 5.8 mm. Designs E and F have a small-to-big width transition at the 3.1 and 1.7 cm mark, respectively. The results of the tests for the fluid flow in both devices are presented in Fig. 14.

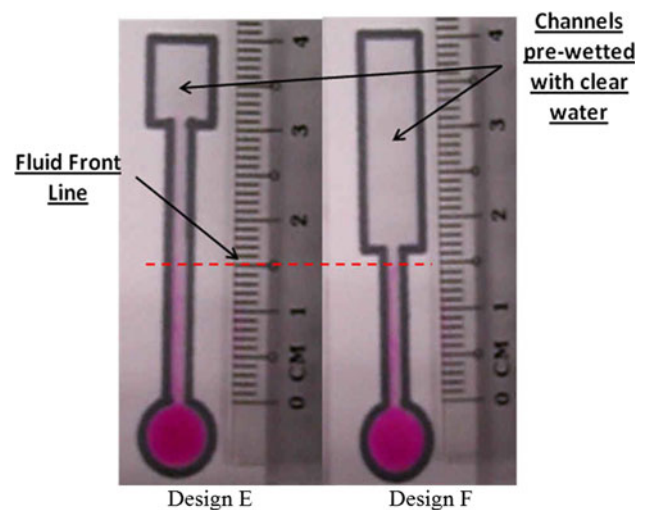


Fig. 13 Flow fronts at the 1.5 cm mark

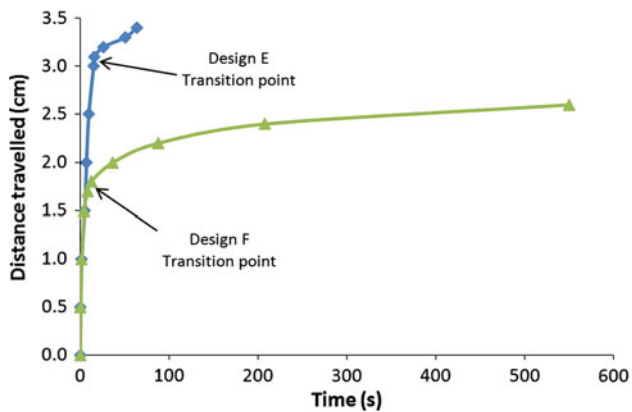


Fig. 14 Flow characteristics for the flow in varying-width channels

The time taken for the fluid front to travel a distance of 1.5 cm from the reservoir is about 5 s in the channels of the two designs. This observation is expected, as the channel widths are the same between the 0 and 1.5 cm marks. However, a deviation in the fluid flow rate begins to surface right after the transition point (i.e., 1.7 cm mark) for design F. The device of design E can transport the fluid further compared to design F, given the same amount of time. This observation is expected, as the volumetric flow rate is assumed to be constant throughout the fluid channels. Hence, as the cross-sectional area increases, the flow rate of the fluid must decrease.

As depicted in Fig. 14, it takes a much longer time for the fluid in the device of design F to be transported the same distance compared to design E. This observation holds as long as the distance travelled passes the transition point for design F. Also evident from the figure, the gradients of the curves are drastically reduced at the transition points for both designs. This implies a reduction in the flow rate of the fluid flowing from a channel with a smaller width to a channel with a larger width.

Experimental results provide a deeper understanding on the flow characteristics in a fully wetted flow. The capillary flow within a channel can be controlled solely by variations in geometric factors. Therefore, there is a possibility of incorporating a system of sequential delivery of reagents in mPADs for various application purposes.

4 Conclusions

Due to its intrinsic hydrophobic nature, wax is capable of channelling the fluid flow within the matrix of a paper substrate. A novel method of using wax as a hydrophobic backing to paper-based devices has been proven feasible through careful and accurate heat treatment. The governing equations for both the wet-out process and fully wetted flow have been proven to be consistent with experimental

results. Deviations from the Washburn equation have been verified in channels with varying geometry. There is possibility of designing a paper-based device that allows accurate manipulation of the fluid and sequential delivery of reagents to various test sites for a variety of applications. Methods of determining properties of paper such as the average pore diameter and permeability have been deduced from experimental results.

Assuming a size of 5 cm × 5 cm paper-device, the total cost including energy consumption for each device can be <US \$0.12. Furthermore, the simplicity in the fabrication and usage steps enables ease of use for the users, thus allowing the possibility of the use of such devices in less developed countries where trained medical personnel may not be readily available. In addition, there is the prospect of potential “use and discard” applications, as the cost of each device is kept to the minimum. These hold great promise in the development of inexpensive mPADs that are able to perform analytical functions in a point-of-care fashion.

References

- Carlen ET, Bomer J, Nieuwkastele van J, Berg van den A (2009) Silicon and glass micromachining. In: Herold KE, Rasooly A (eds) Lab on a chip technology: fabrication and microfluidics. Caister Academic Press, Norfolk, pp 83–114
- Carrilho E, Martinez AW, Whitesides GM (2009) Wax printing, a simple micropatterning process for paper based microfluidics. *Anal Chem* 81(16):7091–7095
- Chartiera I, Sudora J, Fouilleta Y, Sarruta N, Borya C, Gruss A (2003) Fabrication of an hybrid plastic–silicon microfluidic device for high throughput genotyping. *Proc SPIE* 4982:208–219
- Coltro WK, Piccin E, Fracassi da Silva JA, Lucio do Lago C, Carrilho E (2007) A toner-mediated lithographic technology for rapid prototyping of glass microchannels. *Lab Chip* 7(7):931–934
- Coltro WK, de Jesus DP, da Silva JA, do Lago CL, Carrilho E (2010) Toner and paper-based fabrication techniques for microfluidic applications. *Electrophoresis* 31(15):2487–2498
- Fiorini GS, Chiu DT (2010) Disposable microfluidic devices—fabrications, functions and applications. *Anal Chem* 82:3–10
- Ford SM, McCandless A, Liu X, Soper SA (2001) Rapid fabrication of embossing tools for the production of polymeric microfluidic devices for bioanalytical applications. *Proc SPIE* 4560:207–216
- Fu E, Ramsey SA, Kauffman P, Lutz B, Yager P (2011) Transport in two-dimensional paper networks. *Microfluid Nanofluid* 10(1):29–35
- Haiducu M, Rahbar M, Foulds IG, Johnstone RW, Sameoto D, Parameswaran M (2008) Deep-UV patterning of commercial grade PMMA for low-cost, large-scale microfluidics. *J Micro-mech Microeng* 18(11):115029
- Kaleibar A, Rahbar A, Haiducu M, Parameswaran M, Ash M (2010) Patterning of PMMA microfluidic parts using screen printing process. *Proc SPIE* 7593:75930E1–75930E8
- Klasner SA, Price AK, Hoeman KW, Wilson RS, Bell KJ, Culbertson CT (2010) Paper-based microfluidic devices for analysis of clinically relevant analytes present in urine and saliva. *Anal Bioanal Chem* 397(5):1821–1829

- Li X, Tian J, Shen W (2010) Thread as a versatile material for low-cost microfluidic diagnostics. *ACS Appl Mater Interfaces* 2(1):1–6
- Lin G, Lee AP (2010) Microfluidics: an emerging technology for food and health science. *Ann N Y Acad Sci* 1190(1):186–192
- Lu Y, Shi W, Jiang L, Qin J, Lin B (2009) Rapid prototyping of paper-based microfluidics with wax for low-cost, portable bioassay. *Electrophoresis* 30(9):1497–1500
- Martinez AW, Phillips ST, Butte MJ, Whitesides GM (2007) Patterned paper as a platform for inexpensive, low-volume, portable bioassays. *Angew Chem Int Ed* 46(8):1318–1320
- Martinez AW, Phillips ST, Whitesides GM (2008a) Three-dimensional microfluidic devices fabricated in layered paper and tape. *Proc Natl Acad Sci* 105(50):19606–19611
- Martinez AW, Phillips ST, Wiley BJ, Gupta M, Whitesides GM (2008b) FLASH: a rapid method for prototyping paper-based microfluidic devices. *Lab Chip* 8(12):2146–2150
- Martinez AW, Phillips ST, Carrilho E, Thomas SW III, Sindi H, Whitesides GM (2008c) Simple telemedicine for developing regions: camera phones and paper-based microfluidic devices for real-time, off-site diagnosis. *Anal Chem* 80(10):3699–3707
- Martinez AW, Phillips ST, Whitesides GM (2010) Diagnostics for the developing world, microfluidic paper based analytical devices. *Anal Chem* 82:3–10
- Nilsson L, Stenstrom S (1996) A study of the permeability of pulp and paper. *Int J Multiph Flow* 23(1):131–153
- Song Y, Kumar CSSR, Hormes J (2004) Fabrication of an SU-8 based microfluidic reactor on a PEEK substrate sealed by a flexible semi-solid transfer (FST) process. *J Micromech Microeng* 14(7):932–940
- Yeo LP, Ng SH, Wang ZF, Xia HM, Wang ZP, Thang VS, Zhong ZW, de Rooij NF (2010) Investigation of hot roller embossing for microfluidic devices. *J Micromech Microeng* 20(1):015017
- Zhong ZW, Wang ZF, Tan YH (2006) Chemical mechanical polishing of polymeric materials for MEMS applications. *Microelectron J* 37(4):295–301
- Zhong ZW, Shan XC, Yao YC (2010) Investigation of antiadhesive coatings for nanoimprinting lithography. *Mater Manuf Process* 25(7):658–664
- Zhong ZW, Leong MH, Liu XD (2011a) The wear rates and performance of three mold insert materials. *Mater Des* 32(2):643–648
- Zhong ZW, Shan XC, Wong SJ (2011b) Roll-to-roll large-format slot die coating of photosensitive resin for UV embossing. *Microsyst Technol Micro Nanosyst Inf Storage Process Syst* 17(12):1703–1711
- Zhou K, Papautsky I (2007) Optimization of COC hot embossing with soft PDMS tools. *Proc SPIE* 6465:64650R-1–64650R-11